Lidar equation in the second-order approximation for media with strongly forward-peaked scattering phase function

V.V. Veretennikov

Institute of Atmospheric Optics,
Siberian Branch of the Russian Academy of Sciences, Tomsk

Received September 17, 2001

Laser sensing theory with multiple scattering taken into account in the small-angle approximation is used to separate out the component of the lidar signal associated with the first two orders of scattering. For media with a strongly forward-peaked scattering phase function, simple formulas for the doubly scattered signal which take account of the geometrical parameters of the lidar are derived. The role of the diffraction component and the geometrical-optics component of the scattering phase function in the doubly scattered signal is examined. The accuracy of this approximation is estimated as a function of the detector field of view for different optical depths of the scattering layer.

Introduction

The first step in the generalization of atmospheric laser sensing theory for conditions of increased atmospheric turbidity was the double scattering approximation.[1–3] Despite significant recent progress in the solution of laser sensing problems for optically dense media with multiple scattering taken into account, low-order scattering (including polarization) effects are still employed to study propagation of lidar signals.[4,5] Because of the simplicity of the associated analytical description, the lidar equation is widely used to retrieve the optical-microphysical parameters of the medium[6–8] under conditions of relatively low atmospheric turbidity. For coarsely dispersed media with a strongly forward-peaked scattering phase function, an approach is developed here to treat multiple scattering effects in analytical form assuming a small deviation of the sensing beam from the initial direction of propagation (the small-angle approximation[9–12]).

References 11 and 13 provide numerical relationships between the small-angle multiple scattering and single-scattering components of lidar returns as functions of the disperse composition and density of the medium for detectors with a variable field of view (FOV). The data presented in Ref. 11 can be used to estimate quantitatively the conditions of a lidar experiment for which the multiple-scattering background signal will be weak and, hence, the contribution of low scattering orders can be expected to dominate. Under such conditions, the formalism of the small-angle approximation of transfer theory can serve as a convenient basis for further simplification of the lidar equation, allowing a direct decomposition of the lidar signal into components with different orders of scattering. To round out the theory developed in Refs. 11 and 13, an account of low scattering orders should be given a special treatment in the small-angle approximation. Results of this study are the subject of this paper.

1. Geometry of the experiment and the initial lidar equation

Suppose that (a) a medium, characterized by high anisotropy of scattering, occupies the half-space $z > 0$; (b) the source and detector are located in the plane $z = 0$ a distance d apart; (c) their optical axes are parallel; and (d) the detector points in the positive z direction. We also assume a unidirectional point source and a step-function detector response with circular symmetry in the angular and spatial coordinates. Given a pulse $\delta(t)$ with energy W transmitted into the atmosphere, for the viewing geometry considered here the power of the lidar return is given by

$$P(z, d, \gamma_r, R_r) = \pi c W \frac{R_r \gamma_r}{z} \beta_\pi(z) \times \times \int_0^\infty Q(\nu, d, z\gamma_r, R_r)\, \Phi(\nu)\, d\nu, \quad (1)$$

where the kernel of the integral transform

$$Q(\nu, d, z\gamma_r, R_r) = \nu^{-1} J_0(\nu d)\, J_1(\nu z\gamma_r)\, J_1(\nu R_r) \quad (2)$$

is defined as a product of three Bessel functions of the first kind and zeroth $J_0(.)$ and first $J_1(.)$ order; $\Phi(\nu) = F^2(\nu)$, where

$$F(\nu) = \exp[-\tau(z) + g(\nu)], \ \tau(z) = \int_0^z \varepsilon(s) ds; \quad (3)$$

$$g(\nu) = \int_0^z \sigma(z - s)\, \tilde{x}(\nu s)\, ds, \quad (4)$$

0235-6880/01/10 841-07 $02.00

$F(\nu)$ is the optical transfer function (OTF) of the medium, $\varepsilon(z)$, $\sigma(z)$, and $\beta_\pi(z)$ are the extinction, scattering, and backscattering coefficients, which depend on the one spatial coordinate z, and $\tilde{x}(p)$ is the Hankel transform of the small-angle scattering phase function. The lidar parameters include the entrance pupil radius R_r and the FOV γ_r of the receiving system. The derivation of equation (1) and the assumptions for which it is valid are discussed in detail elsewhere.[9,13] Here we only note that equation (1) takes account of small-angle multiple scattering and large-angle single scattering, including backscattering.

2. Approximation of low orders of scattering

We remove the factor $\exp[-2\tau(z)]$ from the function $\Phi(\nu)$ and represent the remaining expression as a series in powers of $2g(\nu)$:

$$\Phi(\nu) = e^{-2\tau(z)} \sum_{n=0}^{\infty} \frac{[2g(\nu)]^n}{n!}. \qquad (5)$$

Then, the zeroth-order term of series (5), $\Phi_0 = e^{-2\tau(z)}$, represents the single-scattering contribution to the lidar return, with the double-scattering contribution being given by

$$\Phi_1(\nu) = 2e^{-2\tau(z)}\, g(\nu). \qquad (6)$$

Generally, the contribution of the $(n+1)$th order of scattering is expressed as

$$\Phi_n(\nu) = e^{-2\tau(z)} \frac{[2g(\nu)]^n}{n!}. \qquad (7)$$

The contribution of higher-than-first orders of scattering to the lidar return is determined by the difference $\Phi_{sc}(\nu) = \Phi(\nu) - \Phi_0$. In the discussion that follows we concentrate on the equation resulting from substitution of two terms of expansion (5) of the function $\Phi(\nu)$ into (1). Physically, this relation expresses the situation in which a photon, on the path from the lidar to the scattering volume where a single scattering has occurred in the backward direction, will suffer not more than one small-angle scattering event.

Substituting $\Phi_0 = e^{-2\tau(z)}$ for $\Phi(\nu)$ in Eq. (1) yields

$$P_1(z, d, \gamma_r, R_r) = \pi c W \frac{R_r \gamma_r}{z} \beta_\pi(z)\, e^{-2\tau(z)} \times \times \int_0^{\infty} Q(\nu, d, z\gamma_r, R_r)\, d\nu. \qquad (8)$$

This is the usual lidar equation in the single scattering approximation with allowance for the geometry of the experiment. The integral of the product of Bessel functions

$$B(d, z\gamma_r, R_r) = \int_0^{\infty} Q(\nu, d, z\gamma_r, R_r)\, d\nu \qquad (9)$$

defines the geometrical lidar factor and is expressed in terms of elementary functions. As shown in Ref. 14, the integral $B(d, z\gamma_r, R_r)$ defined by Eq. (9) is proportional to a two-dimensional convolution of circles with radii R_r and $z\gamma_r$:

$$B(r, z\gamma_r, R_r) = \frac{1}{2\pi R_r z\gamma_r} U_{z\gamma_r}(r) ** U_{R_r}(r), \qquad (10)$$

where $U_a(r)$ is the unit step function in the xy plane

$$U_a(r) = \begin{cases} 1, & 0 \le r < a, \quad r = \sqrt{x^2 + y^2} \\ 0, & r > a \end{cases}. \qquad (11)$$

Since the convolution of two circles is equal to the area of their intersection region, it follows from geometrical considerations that

$$U_a(r) ** U_b(r) = \begin{cases} 0, & r > a + b, \\ \pi a^2, & 0 \le r < |a - b|, \ a < b, \\ \pi b^2, & 0 \le r < |a - b|, \ a > b, \\ a^2\beta + b^2\alpha - ab\sin\gamma, & |a - b| < r < a + b, \end{cases} \qquad (12)$$

where α, β, and γ are the angles in the triangle subtending the sides a, b, and r, respectively. From formulas (10) and (12) it follows that for

$$z > (R_r + d)/\gamma_r \qquad (13)$$

the power of the singly scattered signal is given by the well-known expression

$$P_1(z) = W \frac{c}{2} z^{-2} S_r \beta_\pi(z)\, e^{-2\tau(z)}, \qquad (14)$$

where $S_r = \pi R_r^2$ is the area of the receiving aperture. Condition (13) defines the far sensing zone.

The double-scattering contribution in the small-angle approximation is accounted for by an extra term obtained from the general formula (1) by substituting $\Phi(\nu)$ for $\Phi_1(\nu)$ in (6):

$$P_2(z, d, \gamma_r, R_r) = 2\pi c W \frac{R_r \gamma_r}{z} \beta_\pi(z)\, e^{-2\tau(z)} \times \times G(d, \gamma_r, R_r), \qquad (15)$$

where

$$G(d, \gamma_r, R_r) = \int_0^{\infty} Q(\nu, d, z\gamma_r, R_r)\, g(\nu)\, d\nu. \qquad (16)$$

We now substitute the function $g(\nu)$ into equation (16), with the transform $\tilde{x}(.)$ preliminarily expressed in terms of the scattering phase function $x(\gamma)$. This leads to the following integral representation of the function $G(d, \gamma_r, R_r)$:

$$G(d, \gamma_r, R_r) = 2\pi \int_0^z \sigma(z - s)\, ds \times$$

$$\times \int_0^\infty D(d, s\gamma, R_r, z\gamma_r)\, x(\gamma)\, \gamma d\gamma. \quad (17)$$

Let us discuss in more detail the properties of the weighting function $D(.)$ in the integrand in expression (17). This functions is defined by an improper integral of the product of four Bessel functions of the first kind:

$$D(d, a, b, c) = \int_0^\infty \nu^{-1} J_0(d\nu) J_0(a\nu) J_1(b\nu) J_1(c\nu) d\nu. \quad (18)$$

Reference 15 represents the function $D(d, a, b, c)$ as defined by formula (18) in a form more convenient for practical calculations. Specifically, the representation of $D(d, a, b, c)$ equivalent to formula (18) has the form of a finite integral

$$D(d, a, b, c) = \int_0^{b+c} A(d, r, b)\, A(r, a, c)\, r dr \quad (19)$$

of a product of functions of the form

$$A(r, a, c) = \int_0^\infty J_0(rt)\, J_0(at)\, J_1(ct)\, dt. \quad (20)$$

From a comparison of formulas (18) and (20), it follows that the evaluation of the integral of the product of four Bessel functions reduces to an evaluation of $A(r, a, c)$ as defined by equation (20), i.e., to an evaluation of integrals of products of three Bessel functions. Like $B(r, a, b)$ in equation (10), the integral $A(r, a, c)$ defined by equation (20) can be given a clear physical interpretation. As shown in Ref. 14, $A(r, a, c)$ is proportional to the two-dimensional convolution

$$A(r, a, c) = \frac{1}{2\pi ac}\, U_c(r) \ast\ast \delta(r - a), \quad (21)$$

where $\delta(r)$ is the Dirac delta function. Applying the method of integrating expressions with δ functions in a two-dimensional domain,[16] the convolution in equation (21) can be represented in terms of elementary functions, and the integral $A(r, a, c)$ can finally be written as

$$cA(r, a, c) = \begin{cases} 0, & r \geq a + c, \\ 0, & r \leq |a - c|, \quad a > c, \\ 1, & r \leq |a - c|, \quad c > a, \\ \alpha/\pi, & 0 < |a - c| \leq r \leq a + c, \end{cases} \quad (22)$$

where α is the angle in the triangle with sides r, a, and c subtending the side c:

$$\alpha = \arccos \frac{a^2 + r^2 - c^2}{2ar}. \quad (23)$$

It can be clearly seen that the behavior of the integral $A(r, a, c)$ (20) is determined by the dependence of the angle α (23) on the ratios a/c and r/c. Reference 15 presents values of $\alpha(\xi, \eta)/\pi$ calculated as a function of $\xi = r/c$ for a set of different $\eta = a/c$ values.

Relations (19), (22), and (23) provide a complete solution of the problem of calculating the weighting function $D(d, s\gamma, R_r, z\gamma_r)$ in formula (17) which takes account of the double-scattering contribution to the lidar return. We now consider a few characteristic cases in which the role and importance of some parameters influencing the function $D(d, s\gamma, R_r, z\gamma_r)$ can be estimated.

2.1. Scheme with coincident transmitter and receiver axes

For this scheme, $d = 0$ and according to formulas (19) and (22) the integral $D(d, a, b, c)$ (18) simplifies to

$$D(d = 0, a, b, c) = \frac{1}{b} \int_0^b A(r, a, c)\, r dr = B(b, a, c), \quad (24)$$

where $B(b, a, c)$ is the function described above in the discussion of the single-scattering approximation [see Eqs. (10)–(12)]. As in the single scattering case, we confine ourselves to a consideration of the far sensing zone (13) only. Then, using equations (14), (15), and (17), we obtain the following simple formula for the ratio of the single- to double-scattering signal power, $m_2 = P_2/P_1$:

$$m_2 = 4\pi \int_0^z \sigma(z - s)\, ds \times$$

$$\times \left[\int_0^{r_1/s} x(\gamma)\, \gamma d\gamma + \int_{r_1/s}^{r_2/s} \Omega(s\gamma)\, x(\gamma)\, \gamma d\gamma \right], \quad (25)$$

where

$$r_1 = z\gamma_r - R_r,\ r_2 = z\gamma_r + R_r,$$

$$\Omega(r) = [U_{z\gamma_r}(r) \ast\ast U_{R_r}(r)]/S_r, \quad (26)$$

$\Omega(r)$ is the normalized convolution of circles in a plane, defined by formulas (12), and $S_r = \pi R_r^2$. The function $\Omega(r)$ decreases monotonically from 1 to 0 as r varies from r_1 to r_2. Dividing the γ integration region into two parts as is done in formula (25) is equivalent to splitting the ratio m_2 into two summands:

$$m_2 = m_2' + m_2''. \quad (27)$$

By interchanging the orders of integration in formula (25), the individual terms in formula (27) can be rewritten as

$$m_2' = 4\pi\left[\tau_{sc}(z)\int_0^{\gamma_1} x(\gamma)\,\gamma d\gamma + \int_{\gamma_1}^{\infty} \tau_{sc}(r_1/\gamma)\,x(\gamma)\,\gamma d\gamma\right], \quad (28)$$

$$m_2'' = 4\pi\left[\int_{\gamma_1}^{\gamma_2} x(\gamma)\,\gamma d\gamma \int_{r_1/\gamma}^{z} \Omega(\gamma s)\,\sigma(z-s)\,ds + \int_{\gamma_2}^{\infty} x(\gamma)\,\gamma d\gamma \int_{r_1/\gamma}^{r_2/\gamma} \Omega(\gamma s)\,\sigma(z-s)\,ds\right], \quad (29)$$

where

$$\tau_{sc}(z) = \int_0^z \sigma(s)ds;\ \gamma_1 = \gamma_r - R_r/z,\ \gamma_2 = \gamma_r + R_r/z. \quad (30)$$

Further simplification of formula (25) can be achieved by estimating the influence of the receiving aperture size. As $R_r \to 0$, the integration region in the second integral in brackets in formula (25) shrinks to a point. Therefore it can be expected that for a sufficiently small receiving aperture radius R_r the second summand m_2'' in (27) can be neglected, wherefore we can set $m_2 \approx m_2'$. The numerical estimates presented in Sec. 3 support the validity of this simplification for the receiving aperture areas typically used in lidar sensing applications. We conclude this section by rewriting formulas (28) and (29) for the case where the scattering medium represents a homogeneous layer located a distance H from the lidar and having a constant scattering coefficient σ_0:

$$m_2' = 4\pi\sigma_0\,(z-H)\left[\int_0^{\omega_1} x(\gamma)\,\gamma d\gamma + \omega_1\int_{\omega_1}^{\infty} x(\gamma)\,d\gamma\right], \quad (31)$$

$$m_2'' = 4\pi\sigma_0\left[\int_{\omega_1}^{\omega_2} x(\gamma)\,d\gamma \int_{r_1}^{(z-H)\gamma} \Omega(r)\,dr + \int_{\omega_2}^{\infty} x(\gamma)\,d\gamma \int_{r_1}^{r_2} \Omega(r)\,dr\right], \quad (32)$$

where $\omega_1 = r_1/(z-H)$, $\omega_2 = r_2/(z-H)$, while r_1 and r_2 are given by formulas (26).

2.2. Bistatic scheme in the approximation of small R_r

In the previous section, we already considered the case of a small entrance aperture of the receiving system for the case when the transmitter and receiver axes of the lidar coincide, i.e., when $d = 0$. Here, we generalize the solution for the function m_2 to the case $d \neq 0$. We begin with the general formula (17). In the bistatic sensing scheme for $d \neq 0$ and small R_r, the function $D(d, s\gamma, R_r, z\gamma_r)$, as in the previous section, has a simpler form:

$$D(d, s\gamma, R_r, z\gamma_r) = \frac{R_r}{2}\,A(d, s\gamma, z\gamma_r). \quad (33)$$

This can be proved, for example, by expanding the Bessel function $J_1(b\nu)$ in formula (18) into a Taylor series and retaining only the first term. Then, recalling the definition of the function $A(d, s\gamma, z\gamma_r)$ in (22), we readily obtain the following expression for the function m_2:

$$m_2 = 4\pi\int_0^z \sigma(z-s)\,ds \times \left[\int_0^{\rho_1/s} x(\gamma)\,\gamma d\gamma + \frac{1}{\pi}\int_{\rho_1/s}^{\rho_2/s} \Psi(s\gamma)\,x(\gamma)\,\gamma d\gamma\right], \quad (34)$$

where

$$\rho_1 = z\gamma_r - d,\ \ \rho_2 = z\gamma_r + d;$$

$$\Psi(s\gamma) = \arccos\frac{(s\gamma)^2 + d^2 - (z\gamma_r)^2}{2ds\gamma}. \quad (35)$$

The weighting function $\Psi(\rho)/\pi$ in formula (34) decreases monotonically from 1 to 0 as ρ varies from ρ_1 to ρ_2. The structure of formula (34) is analogous to that of formula (25). Therefore, all subsequent steps in the derivation of formula (34) follow from formulas (27)–(29) and (31), (32) for the function m_2 (25) after substituting ρ_1, ρ_2, and the function $\Psi(\rho)/\pi$ in them for r_1, r_2, and $\Omega(r)$, respectively. In particular, for $d = 0$ we have

$$m_2 = 4\pi\int_0^z \sigma(z-s)\,ds\left[\int_0^{z\gamma_r/s} x(\gamma)\,\gamma d\gamma\right], \quad (36)$$

i.e., exactly the same result as was obtained in the previous section.

3. Numerical results

In this section, results of calculations of the function $m_2(\gamma_r)$ from the formulas of the preceding section are presented, and the accuracy of the considered approximation is estimated as a function of the optical properties of the scattering medium and geometry of the experiment. In all the calculations presented below, the scattering medium is modeled as a homogeneous layer with constant optical characteristics, composed of particles with radius $R = 10$ μm. The calculations were performed for the wavelength $\lambda = 0.55$ μm. The scattering phase function was calculated in the small-angle approximation with the diffraction (D) and geometrical-optics (GO) contributions taken into account separately.[13,17] The experiment is characterized by the following

geometrical parameters: distance between the lidar and the nearest layer boundary $H = 1$ km, range $z = 2$ km, and distance between the optical axes of the source and receiver $d = 0$.

3.1. Influence of the receiving aperture radius

The influence of the receiving aperture radius R_r on the behavior of the function $m_2(\gamma_r)$ is illustrated in Figs. 1 and 2. These dependences were calculated assuming unit optical depth. Figure 1 shows the behavior of the function $m_{2D}(\gamma_r)$ calculated in the diffraction approximation. Curve *1* in Fig. 1 depicts the behavior of the function $m_{2D}(\gamma_r)$ for $R_r = 0$, while curves *2* and *3* describe the function $m_{2D}(\gamma_r)$ and its component $m'_{2D}(\gamma_r)$ (31) for receiving aperture radius $R_r = 0.2$ m. We note that for the z, d, and R_r values considered here, the far zone condition (13) is satisfied for $\gamma_r > 0.2$ mrad. Curves *1* and *2* in Fig. 1 nearly coincide, while $m_{2D}(\gamma_r)$ is dominated by the $m'_{2D}(\gamma_r)$ component.

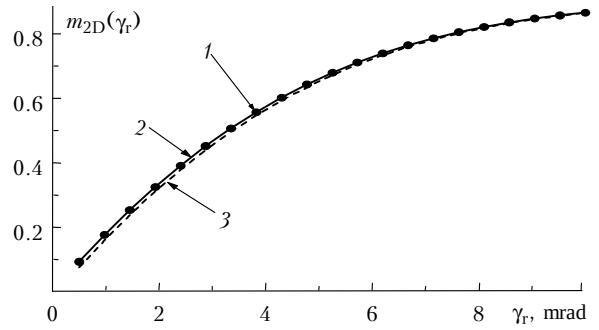

Fig. 1. Dependence of the functions $m_{2D}(\gamma_r)$ (solid line) and $m'_{2D}(\gamma_r)$ (dashed line) on the detector FOV γ_r for $R_r = 0.2$ m and $R_r = 0$ (circles) for a homogeneous layer with optical depth $\tau = 1$.

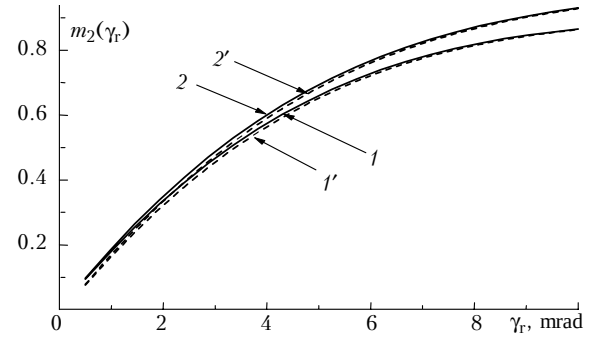

Fig. 2. Influence of receiving aperture size on the dependence $m_2(\gamma_r)$ without (curves *1* and *1′*) and with (curves *2* and *2′*) the geometrical-optics component of the scattering phase function taken into account; curves *1*, *2* depict the functions $m_{2D}(\gamma_r)$ and $m_2(\gamma_r)$ for $R_r = 0$, and curves *1′*, *2′* depict the functions $m'_{2D}(\gamma_r)$ and $m'_2(\gamma_r)$ for $R_r = 0.2$ m.

Figure 2 compares the dependences $m_{2D}(\gamma_r)$ and $m'_{2D}(\gamma_r)$ (curves *1*, *1′*) obtained in the diffraction approximation for $R_r = 0$ and $R_r = 0.2$ m, respectively, with the analogous dependences $m_2(\gamma_r)$ and $m'_2(\gamma_r)$ (curves *2*, *2′*) obtained with the GO contribution to the scattering phase function taken into account. It can be seen from Fig. 2 that the scattering phase function has much greater influence on the accuracy of the $m_2(\gamma_r)$ calculation than the size of receiving aperture. Therefore, $R_r = 0$ will be assumed throughout the subsequent calculations. Taking into account the finding of the previous section that the functions $m_2(\gamma_r)$ have identical analytical descriptions for $R_r \neq 0$ and for $d \neq 0$ when R_r is small, slight departures from $d = 0$ can be neglected.

3.2. Relationship between diffraction and geometrical-optics components of the scattering phase function

We consider in detail the relationship between the contributions of the diffraction component and the geometrical-optics component of the scattering phase function to the function $m_2(\gamma_r)$. The function $m_2(\gamma_r)$, as well as its D and GO components for $\tau = 1$, is plotted in Fig. 3. In the behavior of the function $m_{2D}(\gamma_r)$ (curve *2*), there is an angular region $\gamma_r < 6 - 8$ mrad where this function grows rapidly followed by a slow approach to its saturation level $m_{2D,\infty} = 1$. This component gives the greatest contribution to the total dependence $m_2(\gamma_r)$ (*1*) over the entire range of the detector FOV γ_r. As γ_r decreases, the difference between $m_2(\gamma_r)$ (*1*) and $m_{2D}(\gamma_r)$ (*2*) becomes insignificant, amounting already at $\gamma_r = 10$ mrad, for example, to only 6.5%. Since the D component of the scattering phase function carries information on particle sizes, this fact can be of use in particle size retrieval from lidar returns for appropriately chosen detector FOVs. The component $m_{2GO}(\gamma_r)$ (*3*) becomes significant for large γ_r. However, the larger is γ_r, the greater is the contribution of higher scattering orders; hence the more questionable becomes the validity of this approximation of $m_2(\gamma_r)$ at larger γ_r.

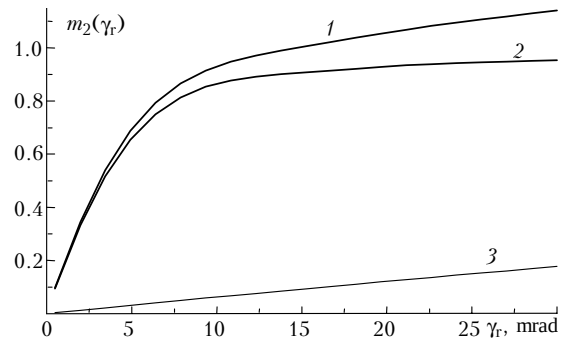

Fig. 3. Separation of the function $m_2(\gamma_r)$ (*1*) into diffraction $m_{2D}(\gamma_r)$ (*2*) and geometrical-optics $m_{2GO}(\gamma_r)$ (*3*) components for a homogeneous layer with optical depth $\tau = 1$.

3.3. Validity estimate as a function of medium density

The most important question in the practical application of this approximation is its error as a function of the optical density of the medium. Obviously, as the turbidity of the medium grows, the contribution of higher scattering orders will also increase, and the rate of this increase will be larger for wider detector FOVs γ_r. For a quantitative estimate of this effect, we compare the dependences of $m_2(\gamma_r)$ obtained in the double-scattering approximation with the function $m(\gamma_r)$ calculated from exact formulas in the small-angle approximation. The comparison is shown in Figs. 4 and 5 for two optical depths, $\tau = 1$ and 2. In the figures, the effects caused by higher scattering orders are compared with the effects of choice of the small-angle scattering phase function. The scattering phase functions used in the comparison differ in that they either include (curves *1* and *2*) or do not include (curves *1′* and *2′*) the GO component. As expected, the contribution of higher scattering orders to the lidar signal increases significantly with increasing detector FOV γ_r, even for a relatively low medium density. This is a more significant factor than choice of the scattering phase function. Nevertheless, as can be seen from the figures, for relatively narrow detector FOVs γ_r, the approximation $m_2(\gamma_r)$ may be quite satisfactory. Usually, this is the case when the total level of multiple scattering in the lidar return is low.

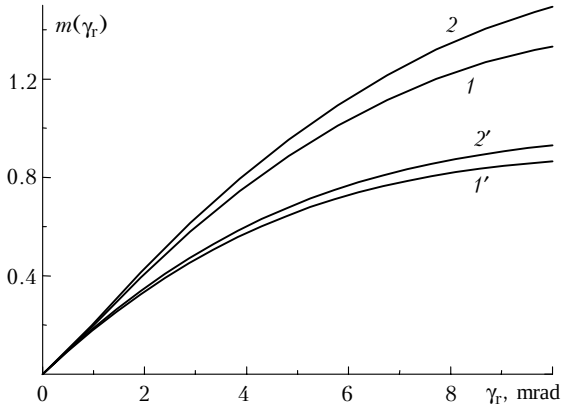

Fig. 4. Comparison of the dependences $m(\gamma_r)$ for the optical depth $\tau = 1$, obtained in the small-angle approximation with all orders of scattering taken into account (curves *1* and *2*) and with the first two orders taken into account (curves *1′* and *2′*); the calculations were performed with the scattering phase function in the diffraction approximation taken into account (curves *1* and *1′*) and with the geometrical-optics component also taken into account (curves *2* and *2′*).

It is useful to estimate the conditions under which the contribution of the first two orders of multiple scattering to the lidar signal are not lower than some preset level. The corresponding dependence of the ratio of the lidar signal power in the double-scattering approximation to the total signal in the small-angle approximation, $\delta_2(\gamma_r) = [P_1(\gamma_r) + P_2(\gamma_r)]/P(\gamma_r)$, is plotted in Fig. 6. From Fig. 6 it can be seen that for the optical depth $\tau \le 1$ the double-scattering contribution makes up over 90% of the total signal power, provided the detector FOV does not exceed 3.4 mrad. As γ_r increases to 8 mrad, the double-scattering contribution decreases to 80%. As the optical depth τ increases to 2, $\delta_2(\gamma_r)$ will remain unchanged only if γ_r is not greater than 2.06 mrad. And finally, for the limiting value considered here, $\tau = 3$, and the limiting level $\delta_2(\gamma_r) = 0.8$, the range of permissible angles γ_r caps off at 1.04 mrad. The estimates presented here are in good agreement with calculations based on other methods (see, e.g., Ref. 18).

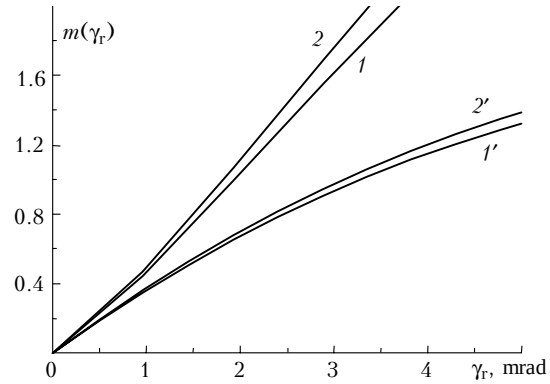

Fig. 5. Comparison of dependences $m(\gamma_r)$ for the optical depth $\tau = 2$, obtained in the small-angle approximation with all orders of scattering taken into account (curves *1* and *2*) and with the first two orders taken into account (curves *1′* and *2′*); the calculations were performed with the scattering phase function in the diffraction approximation taken into account (curves *1* and *1′*) and with the geometrical-optics component also taken into account (curves *2* and *2′*).

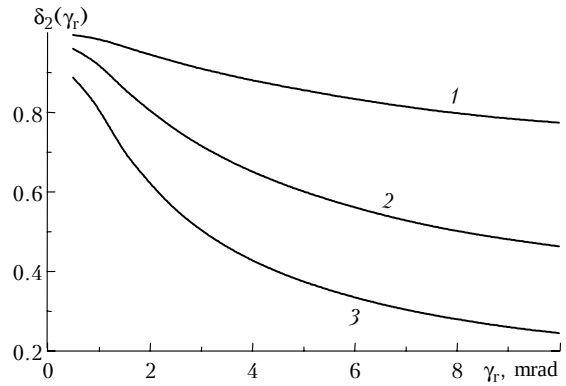

Fig. 6. Relative contributions of the first and second scattering orders to the total lidar signal in the small-angle approximation for optical depths $\tau = 1$, 2, and 3 (curves *1–3*).

The numerical estimates presented here are readily extended to a wider range of situations using similarity properties for the characteristic $m(\gamma_r)$.[11] For the function $m_2(\gamma_r)$, the quantity

$$p = \frac{R}{\lambda}\frac{z}{z-H}\gamma_r \qquad (37)$$

serves as a generalized parameter. For p = const, the function $m_2(\gamma_r)$ keeps constant value. Therefore, a displacement of the layer, for example, while all other parameters are kept fixed, leads to a transformation of $m_2(\gamma_r)$ of the form

$$m_2(z', \gamma_r) = m_2[z, (z'/z)\,\gamma_r]. \quad (38)$$

Similar transformations follow by varying the other parameters entering into formula (37).

Conclusion

Let us summarize the main results and conclusions of this work. Starting from the lidar equation, written with all scattering orders taken into account in the small-angle approximation, we have obtained a specific equation describing the behavior of a lidar signal when only two orders of scattering are taken into account. This equation includes a simple analytical dependence on the small-angle scattering phase function in the form of a linear integral transform. The kernel of this transform is determined by the geometrical parameters of the receiving-transmitting system of the lidar including the entrance pupil radius, detector FOV, and distance between the optical axes of the receiver and transmitter of the lidar. More attention is given to the monostatic sensing scheme with coincident transmitter and receiver axes, as well as the bistatic scheme with parallel receiver and transmitter axes for small receiver aperture size.

For the obtained equation, the influence of different factors is quantitatively estimated, as is its range of validity. As model calculations show, the main geometrical factor influencing the second-order scattered signal is the detector FOV, whereas the size of the receiving aperture can be neglected in many typical cases. Comparison with calculations of the lidar return from exact formulas in the small-angle approximation demonstrates the applicability of the double-scattering approximation for optical depths up to 3 for sufficiently narrow detector FOVs. Here the smallness of the detector FOV is a relative parameter related via similarity relations to the sizes of the scattering particles, distance to the layer, and penetration depth to the layer. For small detector FOVs, for which the approximation considered here gives reasonable results, the lidar signal in the small-angle scattering phase function is influenced mainly by the diffraction component of the phase function.

References

1. E.W. Eloranta, in: *Abstracts of Reports at IV Conference on Laser Radar Studies of the Atmosphere*, Tucson (1972), pp. 25–27.
2. B.V. Kaul and I.V. Samokhvalov, Izv. Vyssh. Uchebn. Zaved., Ser. Radiofizika, No. 8, 109–113 (1975).
3. A. Cohen and M. Graber, Optical and Quantum Electronics **7**, 221–228 (1975).
4. V.V. Bryukhanova and I.V. Samokhvalov, Proc. SPIE **4341**, 358–361 (2000).
5. S.V. Samoilova, Atmos. Oceanic Opt. **14**, No. 3, 161–167 (2001).
6. Y. Benayahu, A. Ben-David, S. Fastig, and A. Cohen, Appl. Opt. **34**, No. 9, 1569–1578 (1995).
7. C. Maby and O. Lado-Bordowsky, *Proc. of MUSCLE10*, Florence, Italy (1999), pp. 227–236.
8. G. Roy, L. Bissonnette, C. Bastille, and G. Vallee, Appl. Opt. **38**, No. 24, 5202–5211 (1999).
9. L.S. Dolin and V.A. Savel'ev, Izv. Akad. Nauk SSSR, Ser. Fiz. Atmos. Okeana **7**, No. 5, 505–510 (1971).
10. E.P. Zege, I.L. Katsev, and I.N. Polonski, Izv. Ros. Akad. Nauk, Ser. Fiz. Atmos. Okeana **34**, No. 1, 45–50 (1998).
11. V.V. Veretennikov, Atmos. Oceanic Opt. **12**, No. 5, 369–375 (1999).
12. V.V. Veretennikov, Atmos. Oceanic Opt. **14**, No. 1, 37–43 (2001).
13. V.E. Zuev, V.V. Belov, and V.V. Veretennikov, *Systems with Applications to Scattering Media* (Publishing House of the Tomsk Affiliate of the SB RAS, Tomsk, 1997), 402 pp.
14. V.V. Veretennikov, Atmos. Oceanic Opt. **11**, No. 9, 858–862 (1998).
15. V.V. Veretennikov, Atmos. Oceanic Opt. **11**, No. 10, 889–894 (1998).
16. A. Papoulis, *Systems and Transforms with Applications in Optics* (McGraw-Hill, New York, 1968).
17. E.P. Zege and A.A. Kokhanovsky, Appl. Opt. **33**, No. 27, 6547–6554 (1994).
18. B.V. Kaul, G.M. Krekov, and M.M. Krekova, Kvant. Elektron. **4**, No. 11, 2408–2413 (1977).